Earth and Planetary Science Letters 366 (2013) 83–98

Contents lists available at SciVerse ScienceDirect

Earth and Planetary Science Letters

journal homepage: www.elsevier.com/locate/epsl

Reconstructing the geometry of central Anatolia during the late Cretaceous: Large-scale Cenozoic rotations and deformation between the Pontides and Taurides

Côme Lefebvre [a,b,*], Maud J.M. Meijers [b,c], Nuretdin Kaymakci [d], Ahmet Peynircioğlu [c], Cor G. Langereis [c], Douwe J.J. van Hinsbergen [e]

[a] Structural Geology and Tectonics Group, Department of Earth Sciences, Faculty of Geosciences, Utrecht University, Budapestlaan 4, 3584 CD Utrecht, The Netherlands
[b] Géoazur, UMR 7329, Université de Nice Sophia Antipolis, Observatoire de la Côte d'Azur, Parc Valrose, 06108 Nice, France
[c] Paleomagnetic Laboratory 'Fort Hoofddijk', Department of Earth Sciences, Faculty of Geosciences, Utrecht University, Budapestlaan 4, 3584 CD Utrecht, The Netherlands
[d] Department of Geological Engineering, Middle East Technical University, 06531 Ankara, Turkey
[e] Physics of Geological Processes, University of Oslo, Sem Sælands vei 24, NO-0316 Oslo, Norway

ARTICLE INFO

Article history:
Received 14 June 2012
Received in revised form
2 January 2013
Accepted 4 January 2013
Editor: T.M. Harrison

ABSTRACT

The Central Anatolian Crystalline Complex (CACC) exposes metamorphic, ophiolitic and igneous rocks that were formed and deformed during closure of the Neotethyan ocean. The CACC is located in central Turkey, between the Pontides in the north and the Taurides in the south, separated by major fault zones. Composite plutons intruded the meta-sedimentary and ophiolitic units between ~95 and 75 Ma, and form linear magmatic belts (~100 km long) along the western and northern margins of the CACC. Exhumation of the metamorphic and igneous complex was finalized by the Paleocene time. In this

Outline

- Description of the Central Anatolian Crystalline Complex (CACC)
- Paleomagnetic studies of fifteen upper Cretaceous plutons
- Three different domains
- Rotations accommodated by two transpressional fault zones
- Deformation caused by collision of the CACC with the Pontides

Tethys Ocean

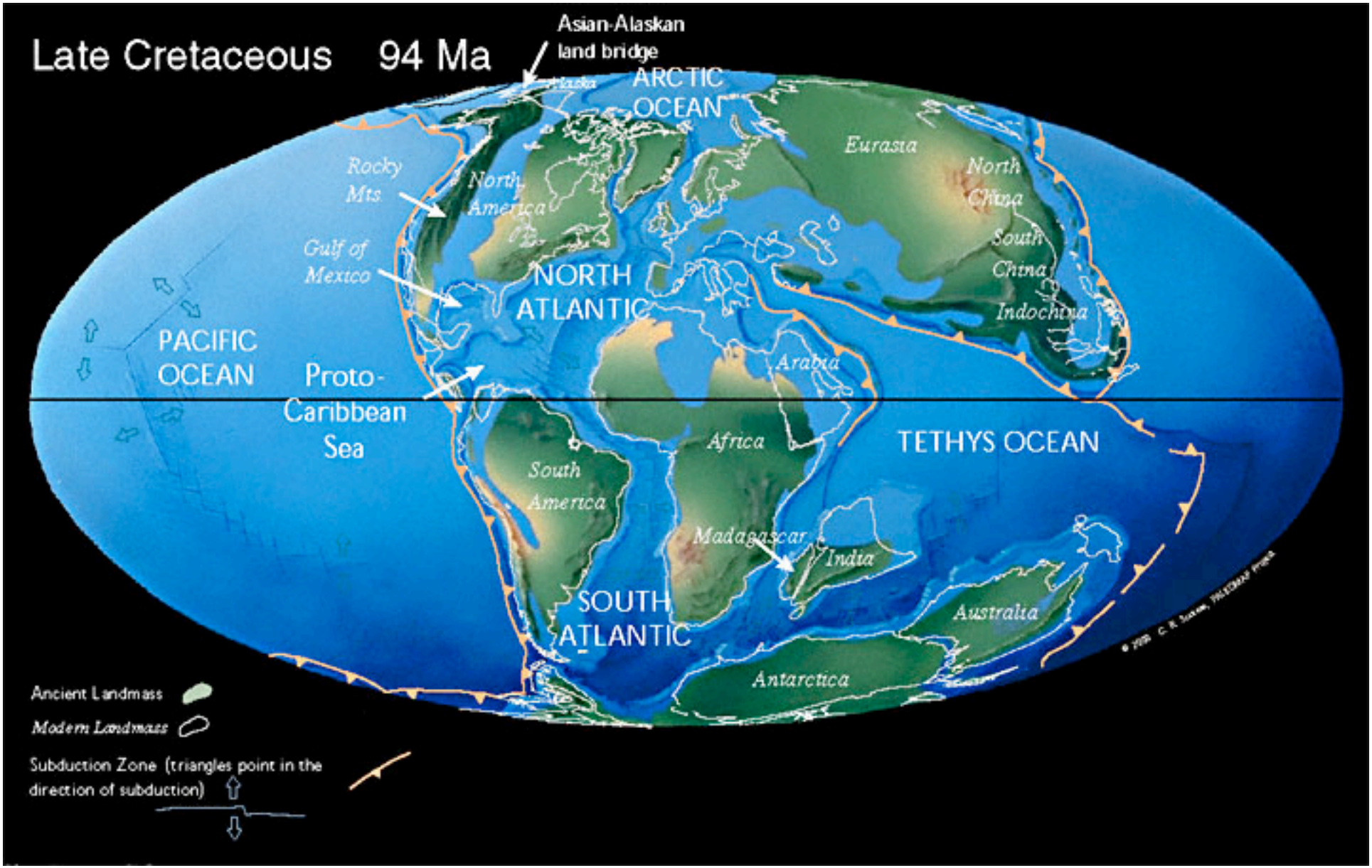

Location of the CACC

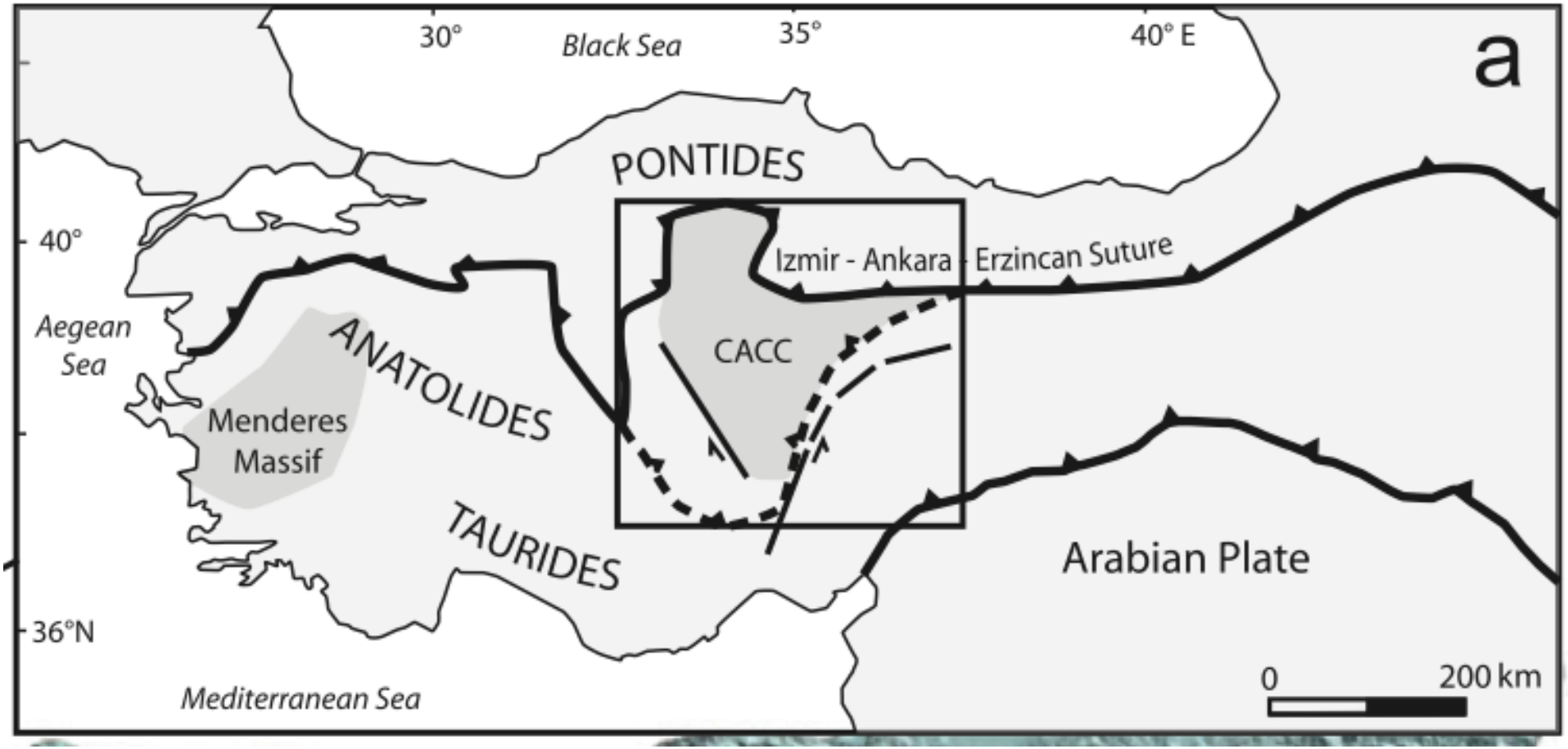

Lefebvre et al. (2013)

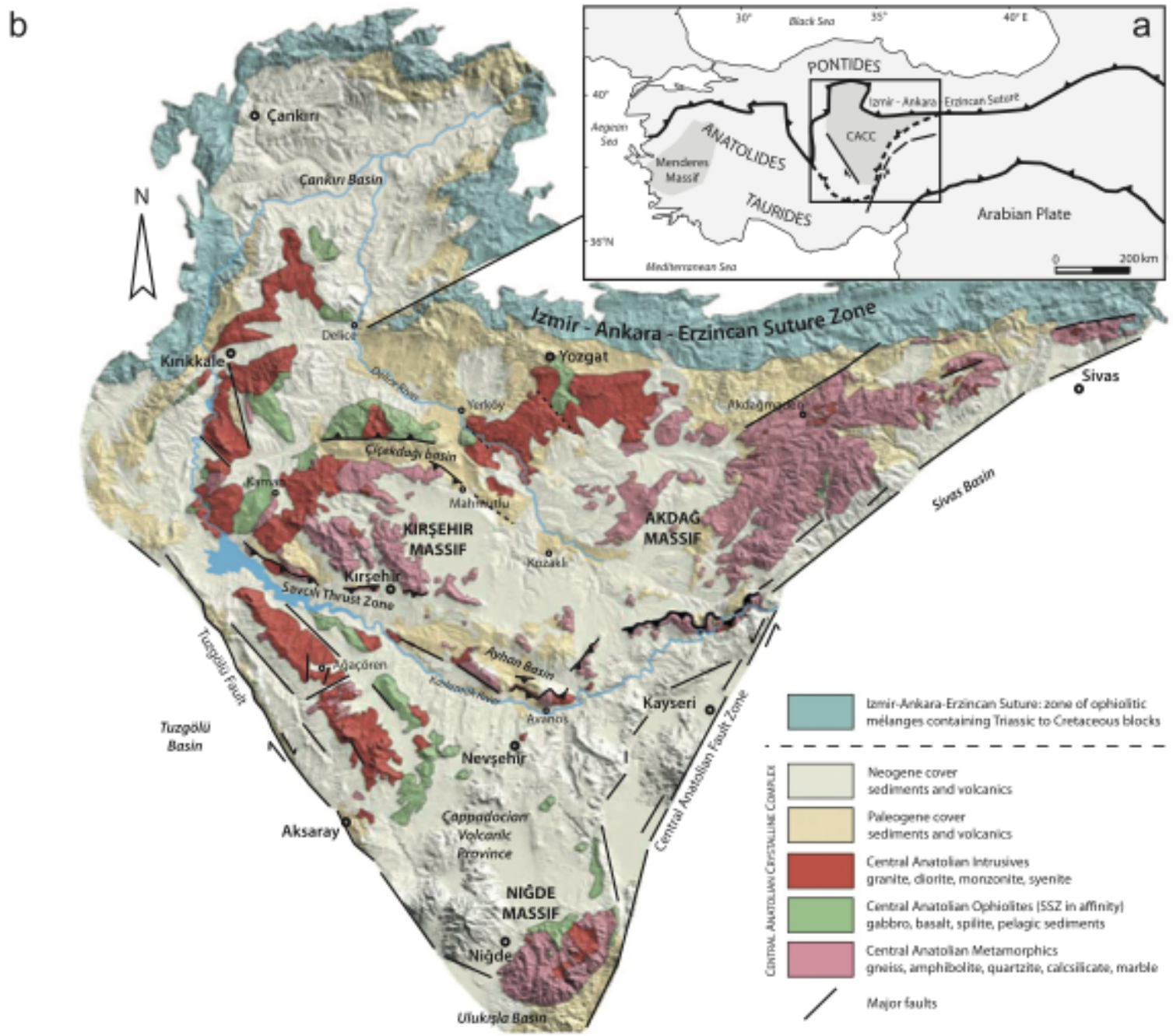
b
a
30°
Black Sea
35°
40° E
PONTIDES
40°
Aegean Sea
ANATOLIDES
Menderes Massif
TAURIDES
Izmir - Ankara
Erzincan Suture
CACC
Arabian Plate
35°N
Mediterranean Sea
0
200 km
N
Çankırı
Çankırı Basin
Izmir - Ankara - Erzincan Suture Zone
Delice
Kırıkkale
Yozgat
Sivas
Delice River
Yerköy
Akdağmadeni
Çiçekdağı basin
Kırıkkale
Mahmutlu
Sivas Basin
KIRŞEHIR MASSIF
AKDAĞ MASSIF
Kozaklı
Kırşehir
Savcılı Thrust Zone
Tuzgölü Fault
Ağaçören
Aybastı Basin
Kızılırmak River
Kayseri
Tuzgölü Basin
Avanos
Nevşehir
Central Anatolian Fault Zone
Aksaray
Cappadocian Volcanic Province
NIĞDE MASSIF
Niğde
Ulukışla Basin
Izmir-Ankara-Erzincan Suture: zone of ophiolitic mélanges containing Triassic to Cretaceous blocks
CENTRAL ANATOLIAN CRYSTALLINE COMPLEX
Neogene cover
sediments and volcanics
Paleogene cover
sediments and volcanics
Central Anatolian Intrusives
granite, diorite, monzonite, syenite
Central Anatolian Ophiolites (SSZ in affinity)
gabbro, basalt, spilite, pelagic sediments
Central Anatolian Metamorphics
gneiss, amphibolite, quartzite, calcsilicate, marble
Major faults

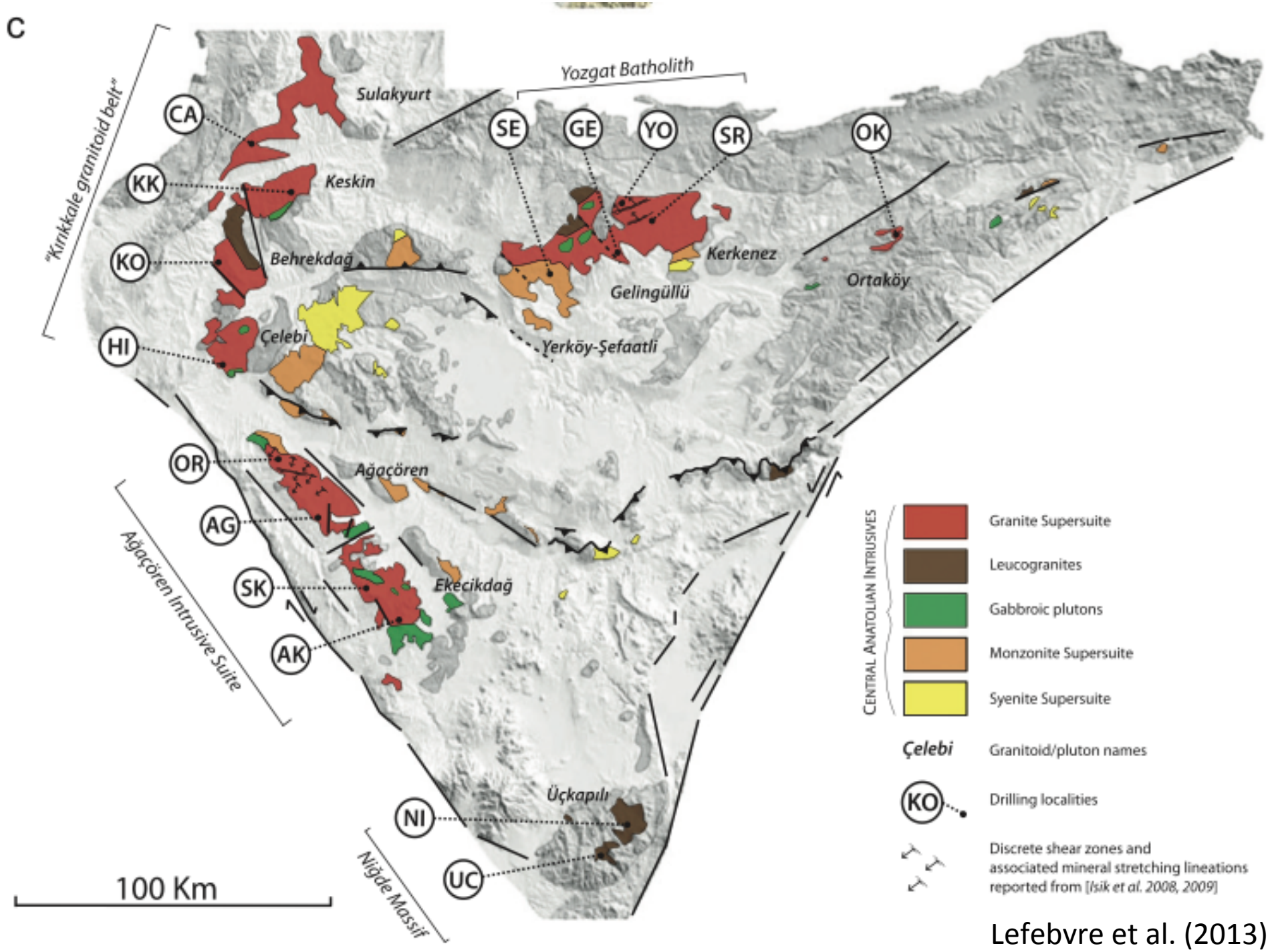

Lefebvre et al. (2013)

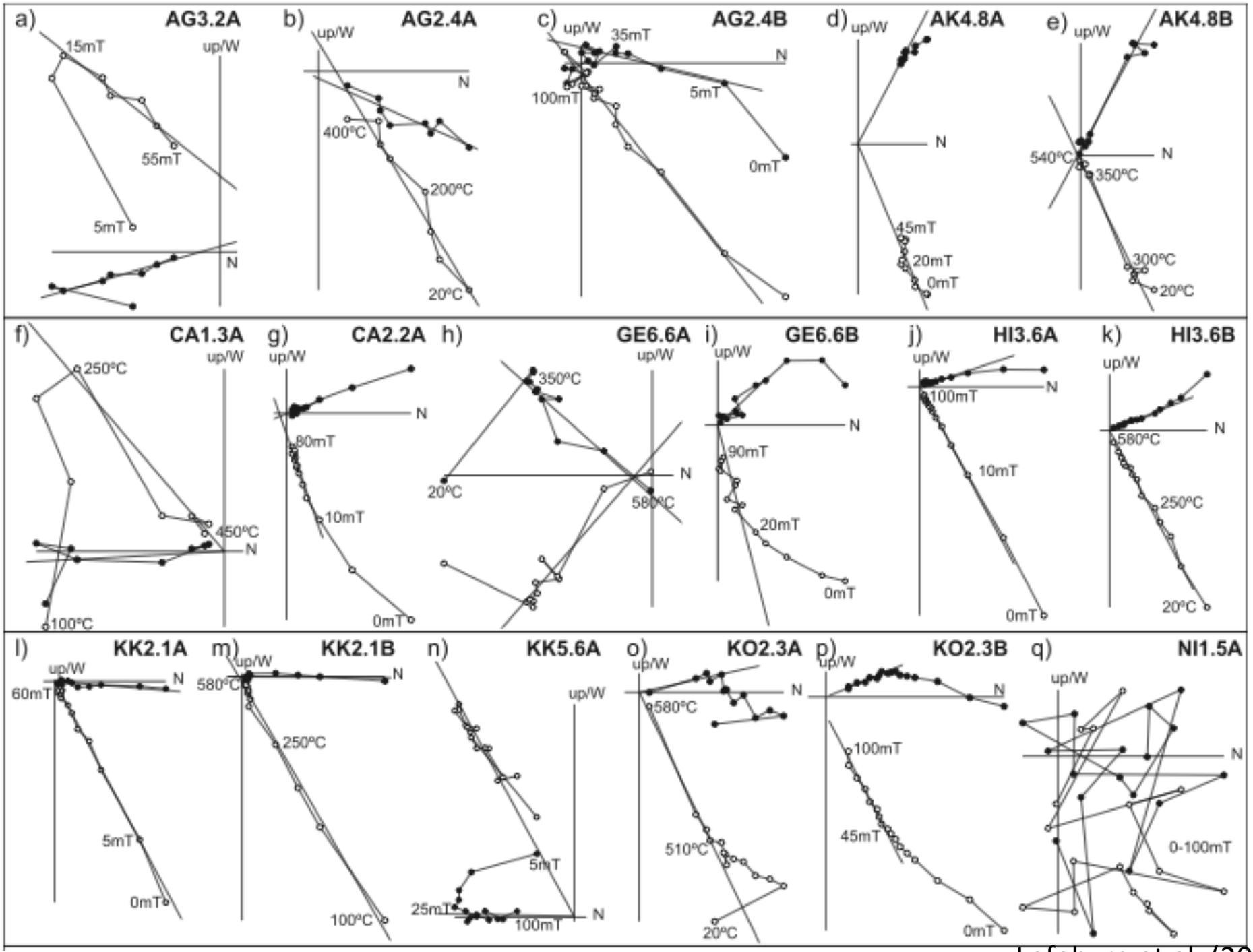

Lefebvre et al. (2013)

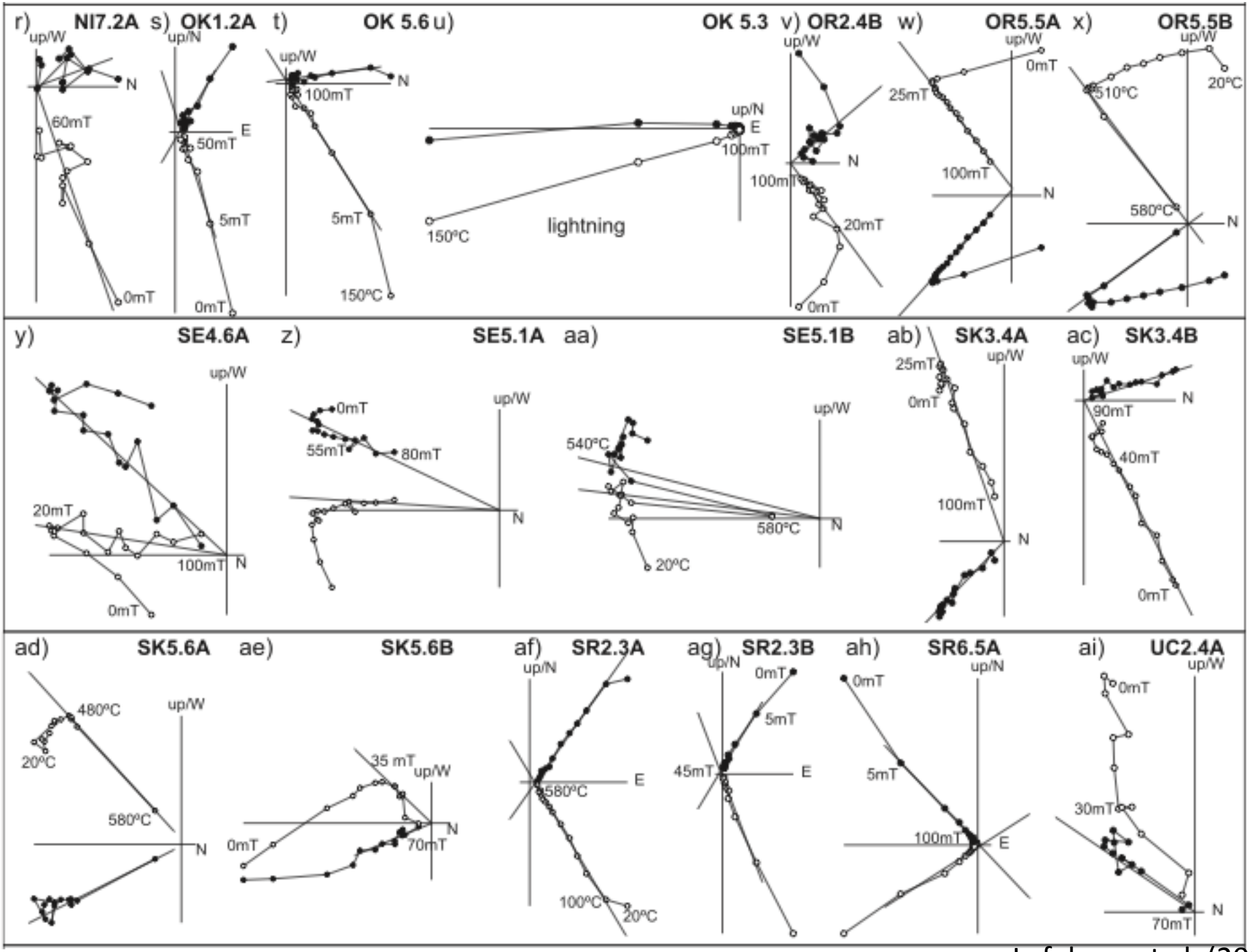

Lefebvre et al. (2013)

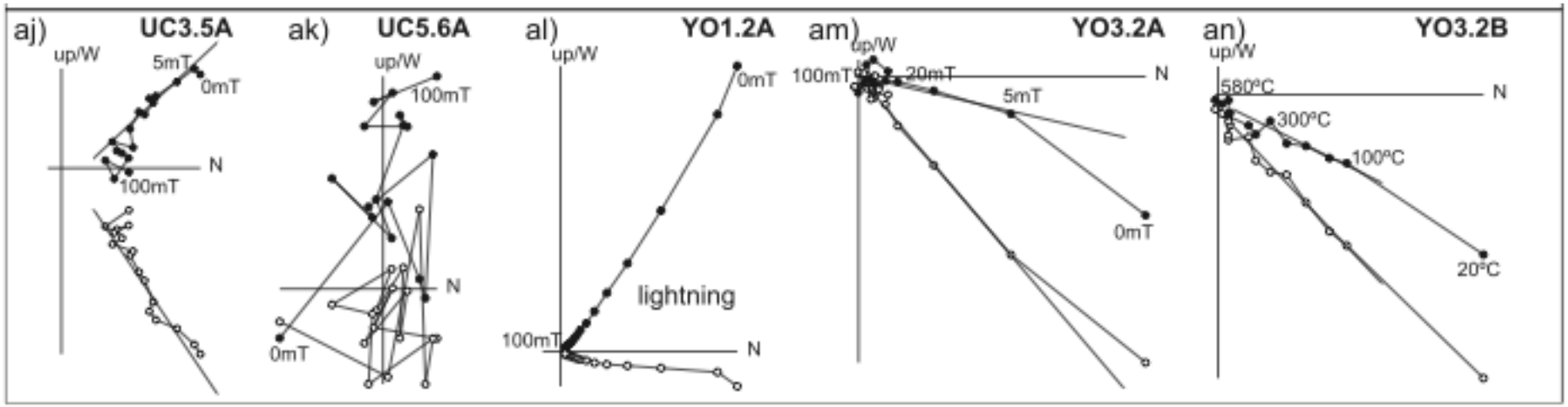

Lefebvre et al. (2013)

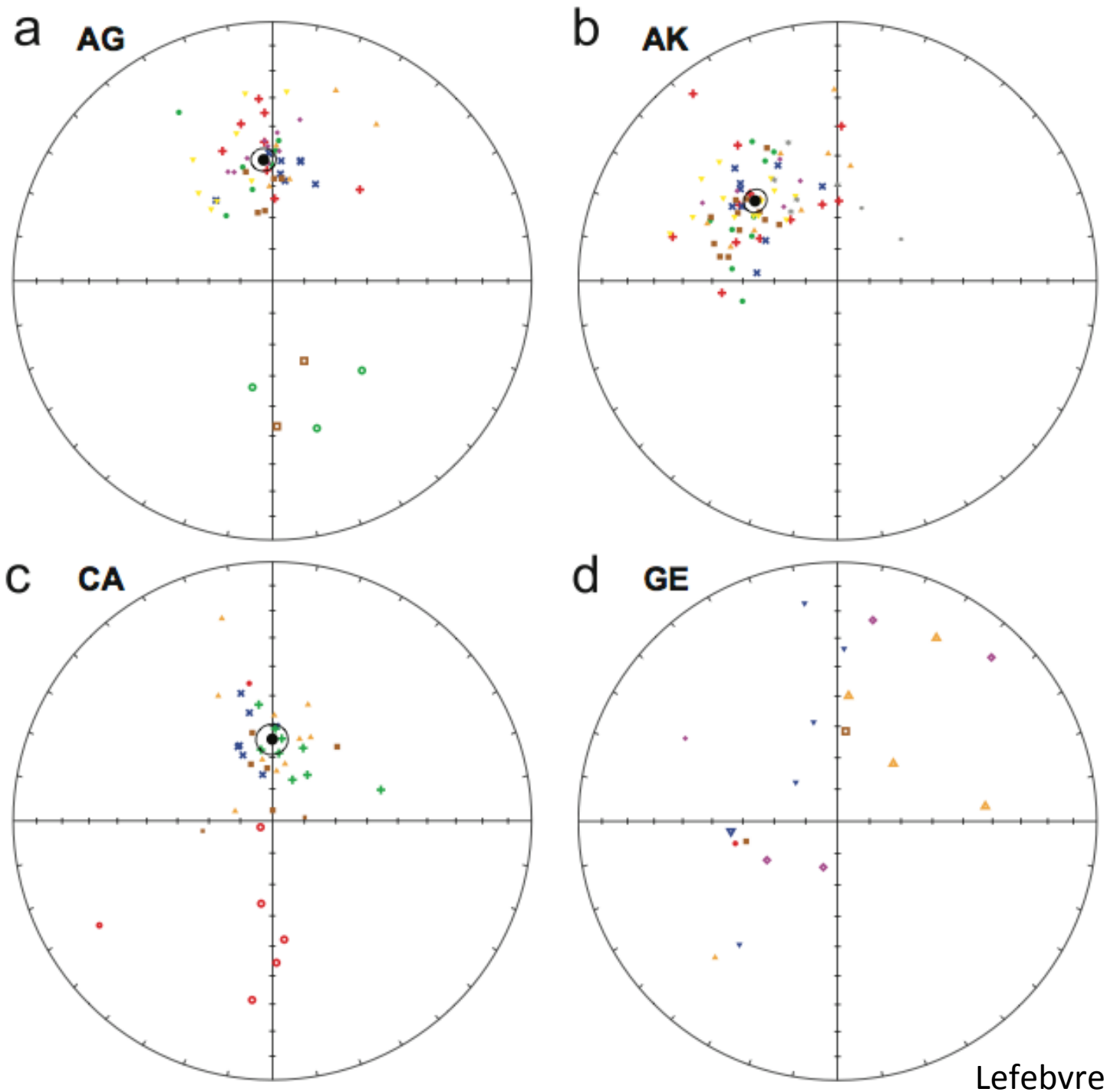

Lefebvre et al. (2013)

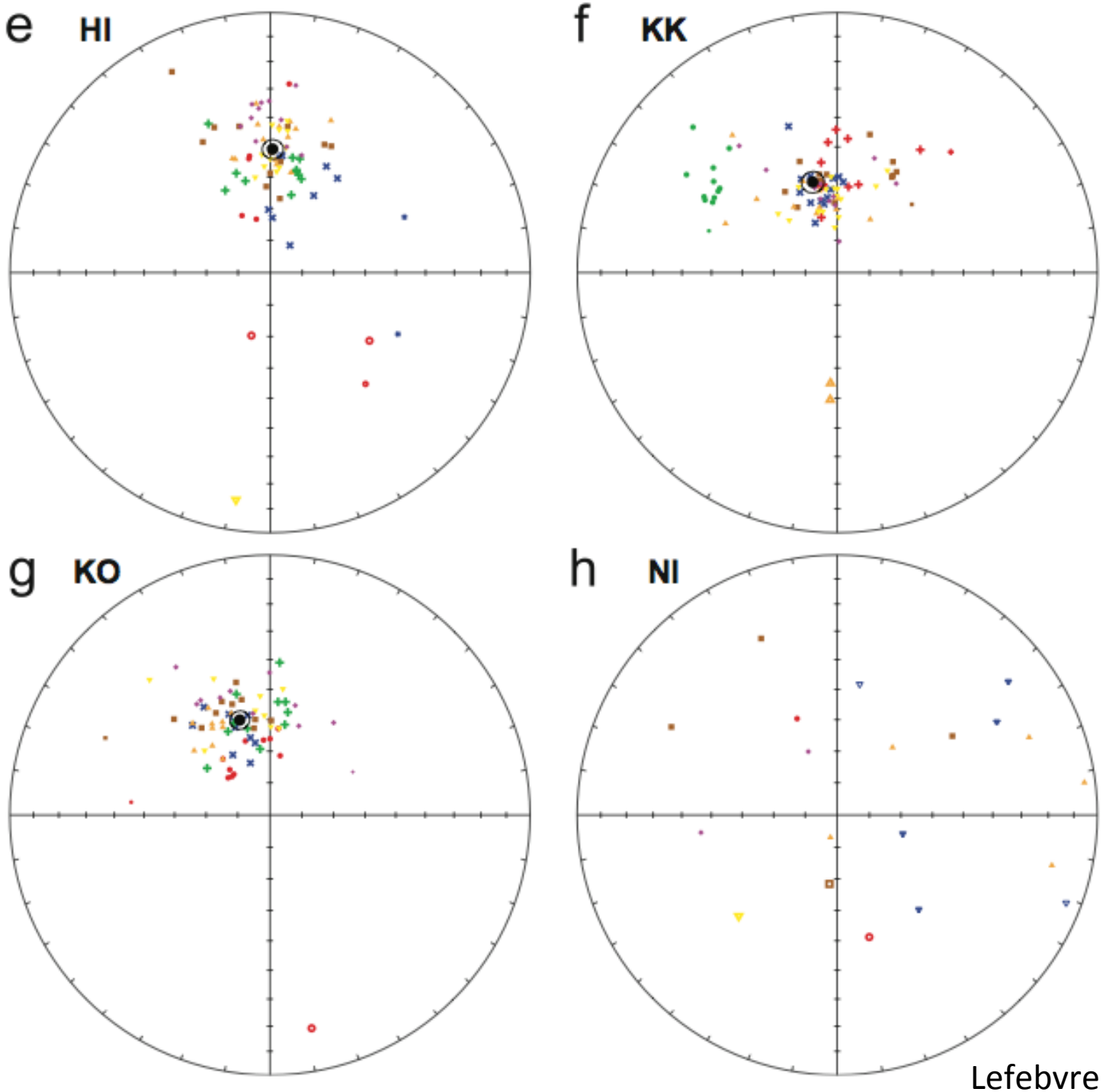

Lefebvre et al. (2013)

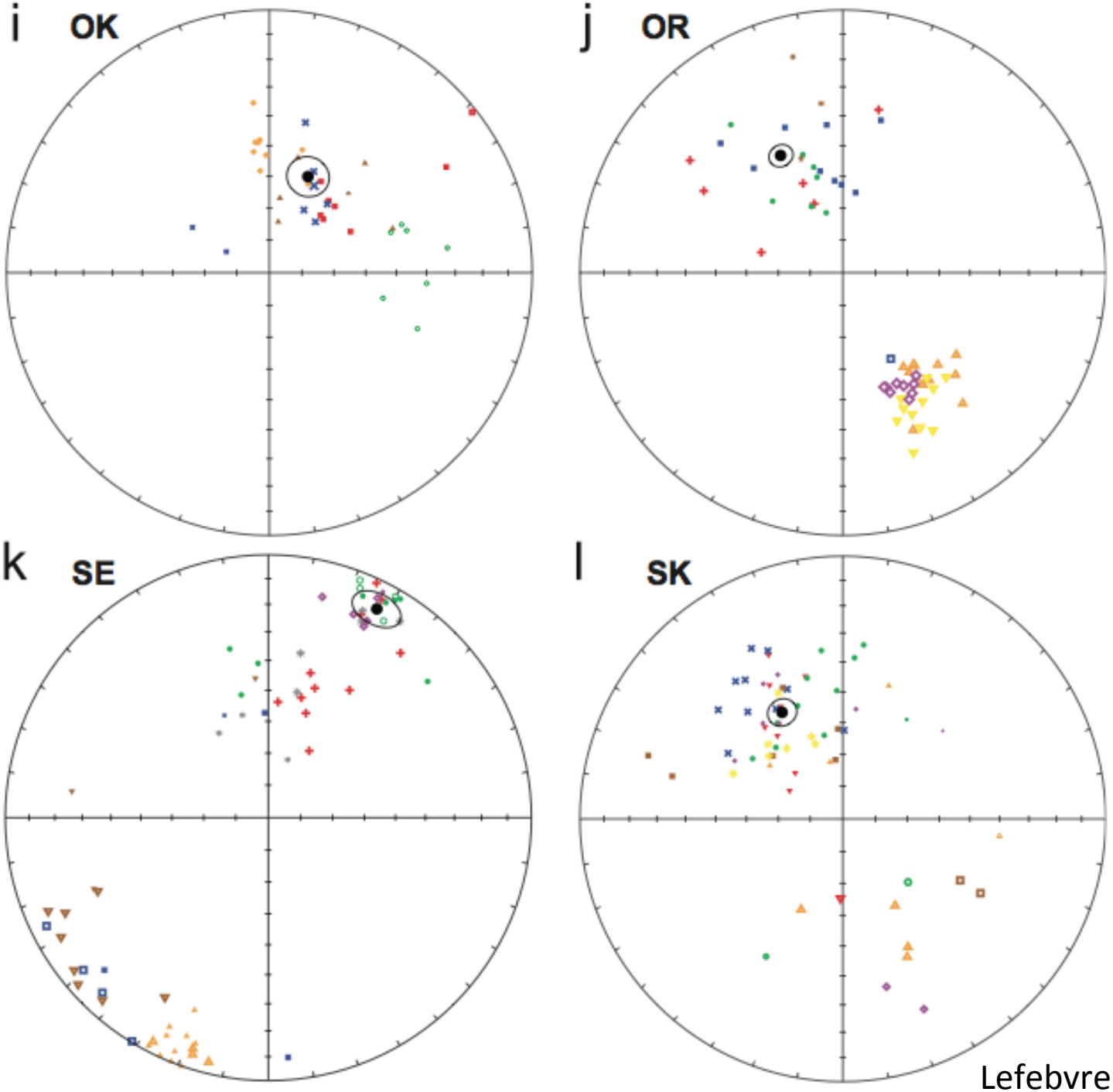

Lefebvre et al. (2013)

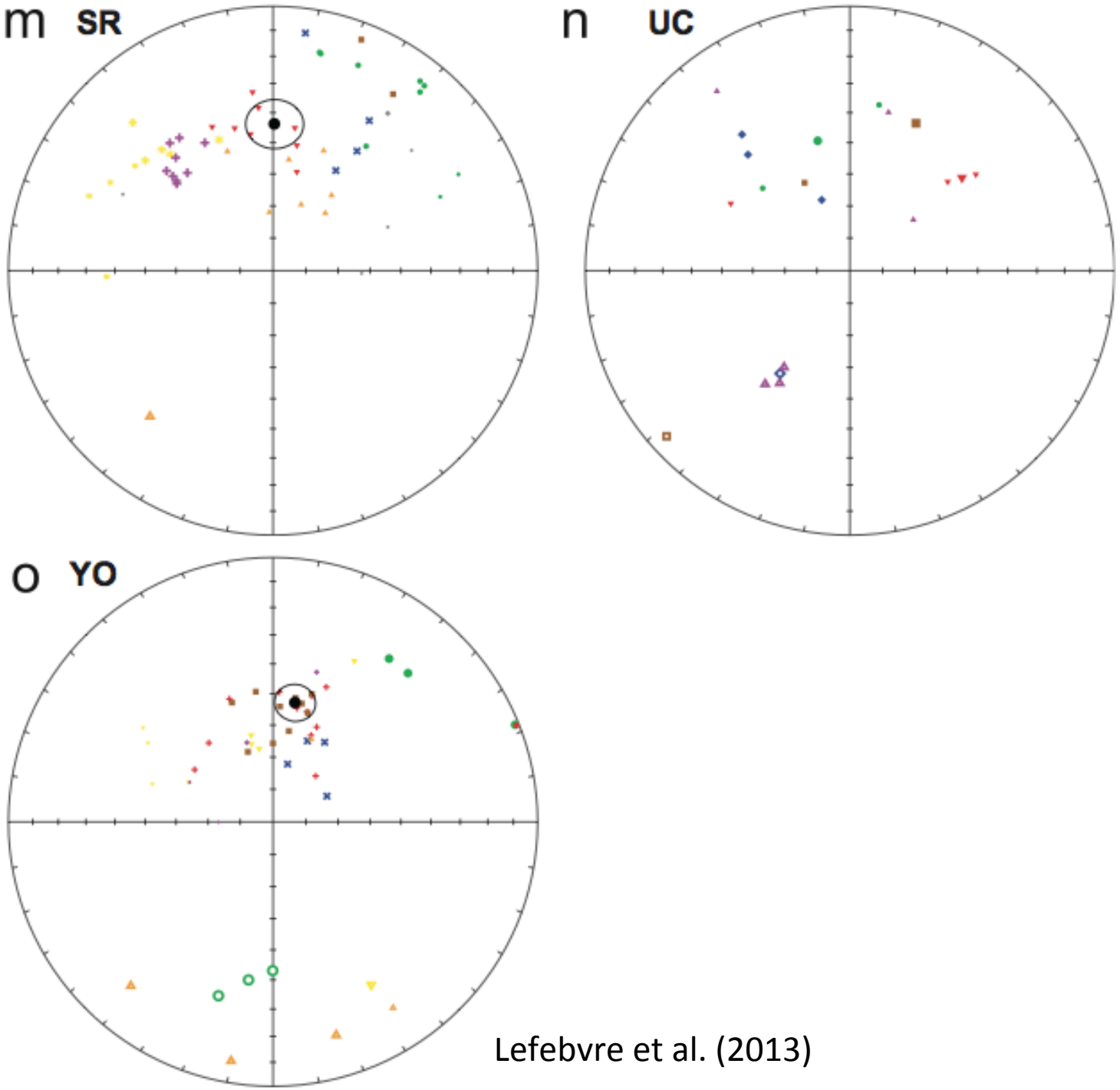

Lefebvre et al. (2013)

Location Means

Table 2(a)
All calculated means per locality and their statistical parameters.

Site	N_{sites}	N_{cores}	N_{demag}	N_a	N_{45}	D	I	λ	ΔD_x	ΔI_x	$K_{(vgp)}$	$A95_{(vgp)}$	$A95_{min}$	$A95_{max}$
AG	7	55	75	55	55	355.4	50.8	31.5	4.6	4.7	21.4	4.2	3.4	6.6
AK	8	60	84	76	74	314.4	53.0	33.6	5.3	4.6	15.1	4.4	3.0	5.4
CA	5	41	43	40	37	359.1	63.8	45.5	9.3	5.2	14.1	6.5	4.0	8.4
GE	7	51	53			No averages calculated								
HI	7	54	79	77	74	0.8	50.8	31.5	4.1	3.8	23.4	3.5	3.0	5.4
KK	7	50	93	89	86	344.3	60.5	41.5	5.9	3.8	13.1	4.4	2.9	5.0
KO	7	57	81	74	71	341.7	58.2	38.9	4.8	3.4	21.6	3.7	3.1	5.6
NI	7	46	46			No averages calculated								
OK	5	41	41	36	26	22.6	57.5	38.1	10.1	7.4	13.9	7.9	4.6	10.5
OR	7	51	75	59	59	331.9	48.3	29.3	4.5	4.5	23.1	3.9	3.3	6.3
SE	7	49	71	71	65	27.5	11.5	5.8	4.9	9.5	13.9	4.9	3.1	5.6
SK	7	55	79	64	60	329.8	51.4	32.1	6.0	5.5	14	5.1	3.3	6.2
SR	8	64	69	54	44								3.7	7.6
UC	7	57	57			No averages calculated								
YO	7	52	76	49	40	9.8	52.0	32.6	7.6	6.8	13.3	6.4	3.9	8.0
OK+YO (AYB)					66	14.5	54.4	34.9	6.2	5.1	12.9	5.1	3.2	5.9
CA+KK+KO+HI (KKB)					268	350.7	57.9	38.6	3.0	2.1	14.8	2.3	1.8	2.4
CA+KK+HI (KKB)					197	353.9	57.7	38.3	3.6	2.6	14	2.8	2.1	2.9
OR+SK+AK+AG (AAB)					248	331.6	51.9	32.5	3.1	2.8	12.7	2.6	1.9	2.5
OR+SK+AK (AAB)					193	324.8	51.3	32.0	3.2	3.0	14.8	2.7	2.1	3.0

N_s=number of sites per locality, N_{cores}=number of sampled cores, N_{demag}=number of demagnetized specimens, N_a=number of interpreted specimens, N_{45}=number of specimens included in the calculation for the mean ChRM direction after applying the 45° fixed cut-off (see Supplementary data for details per site), dec=declination, inc=inclination, λ=paleolatitude, ΔD_x (ΔI_x)=error in declination (inclination)calculated from the A95, $K_{(VGP)}$=precision parameter determined from the mean virtual geomagnetic pole directions (VGPs), $A95_{(VGP)}$=cone of confidence determined from the mean VGP direction, and $A95_{min}$ ($A95_{max}$)=minimum (maximum) value of the A95 for the given dataset based on Deenen et al. (2011). The strikethrough numbers of locality SR correspond to the value which does not pass the criteria $A95_{min} < A95 < A95_{max}$.

Lefebvre et al. (2013)

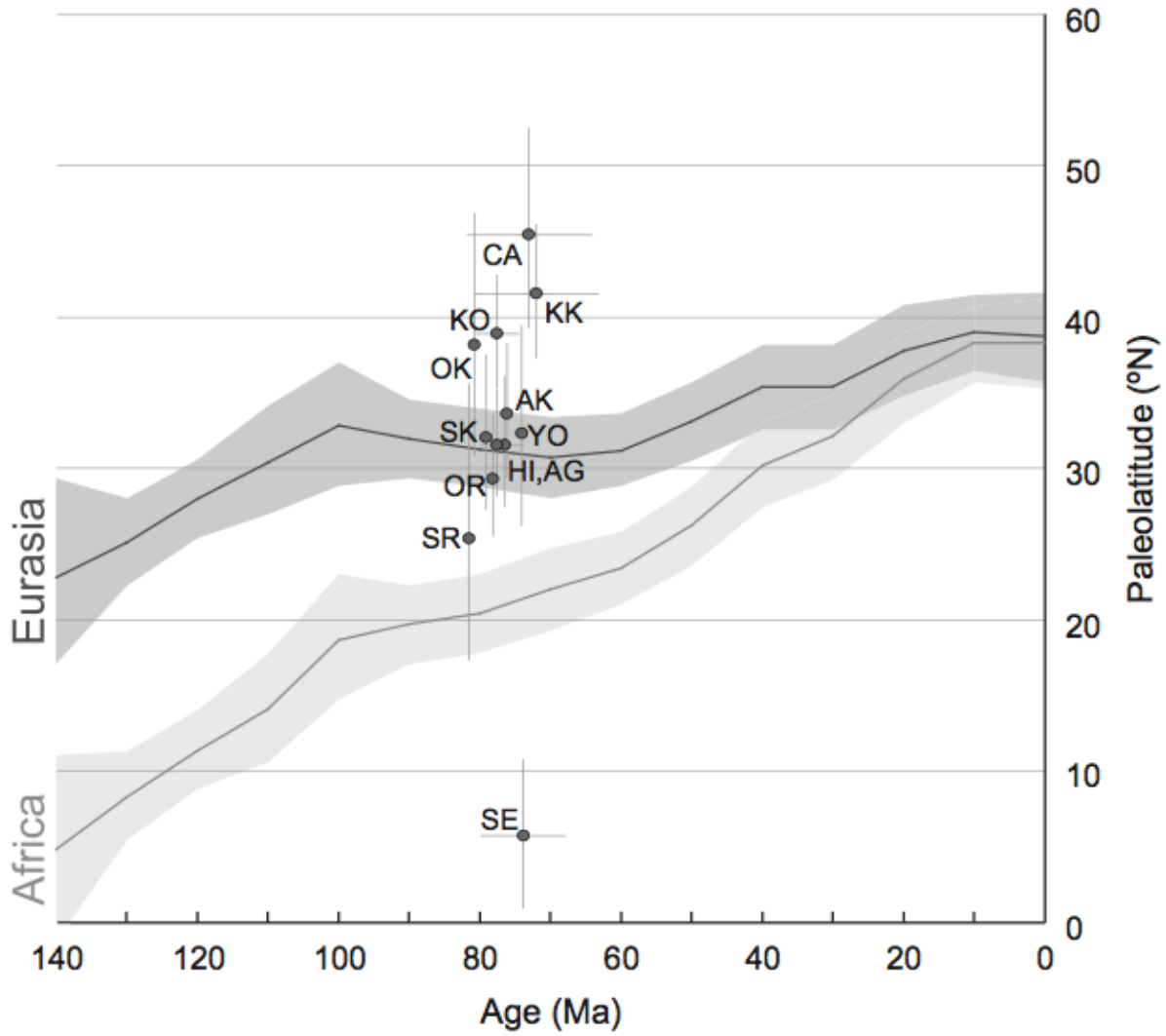

Fig. 4. Age versus latitude plot showing the curves for Africa and Eurasia calculated from the APW paths (Torsvik et al., 2008) with their $\Delta\lambda$ error (using the ΔI_x calculated from A95, shaded area). Calculated paleolatitudes from the accepted localities are plotted with their $\Delta\lambda$ error (calculated from the ΔI_x). The available isotopic ages used in the plot are the ones marked with an asterisk in Table 1; the choice of the age for the undated granitoids is explained in Section 4.1 (paleomagnetic results). Some ages were slightly shifted for the purpose of better display.

Lefebvre et al. (2013)

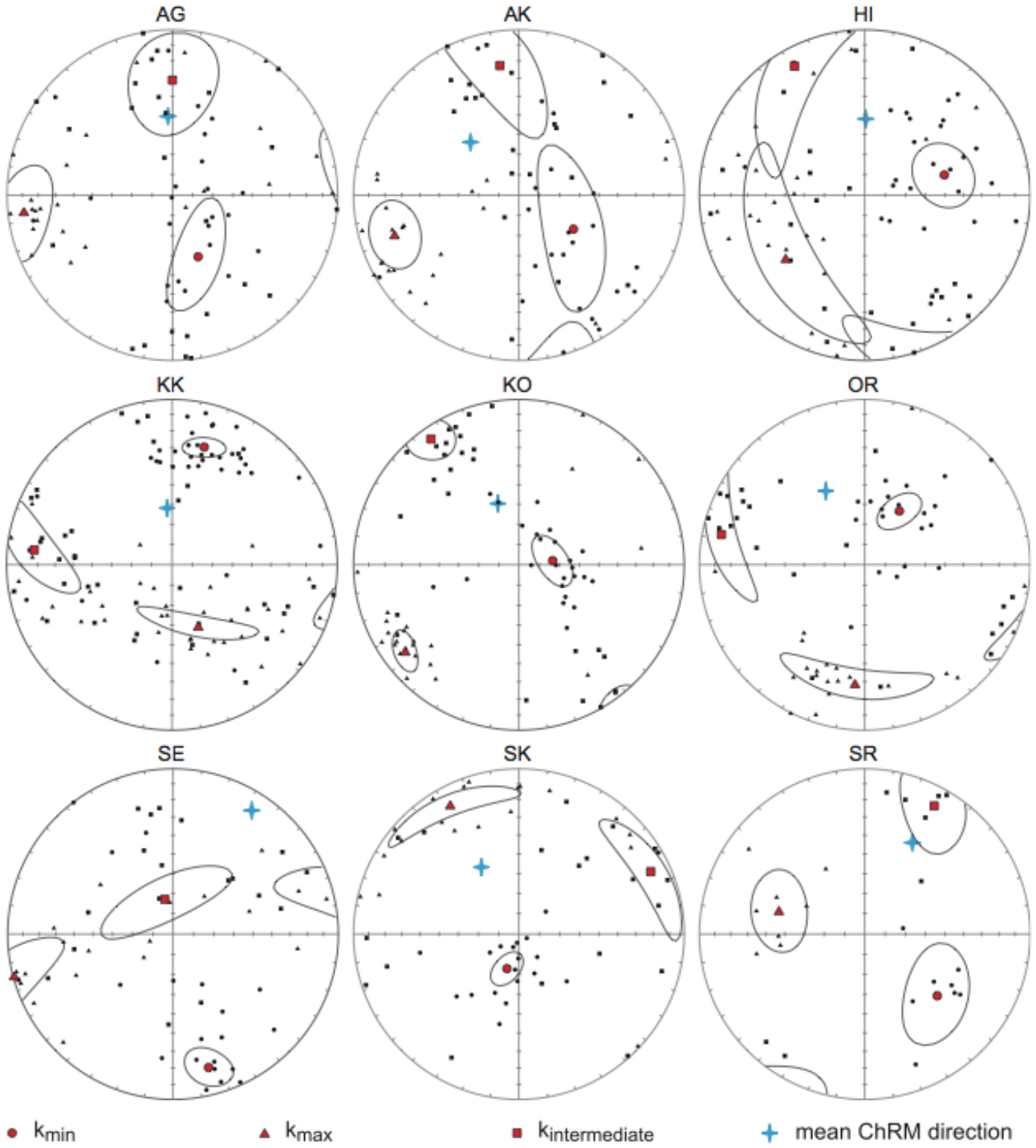

Lefebvre et al. (2013)

Lefebvre et al. (2013)

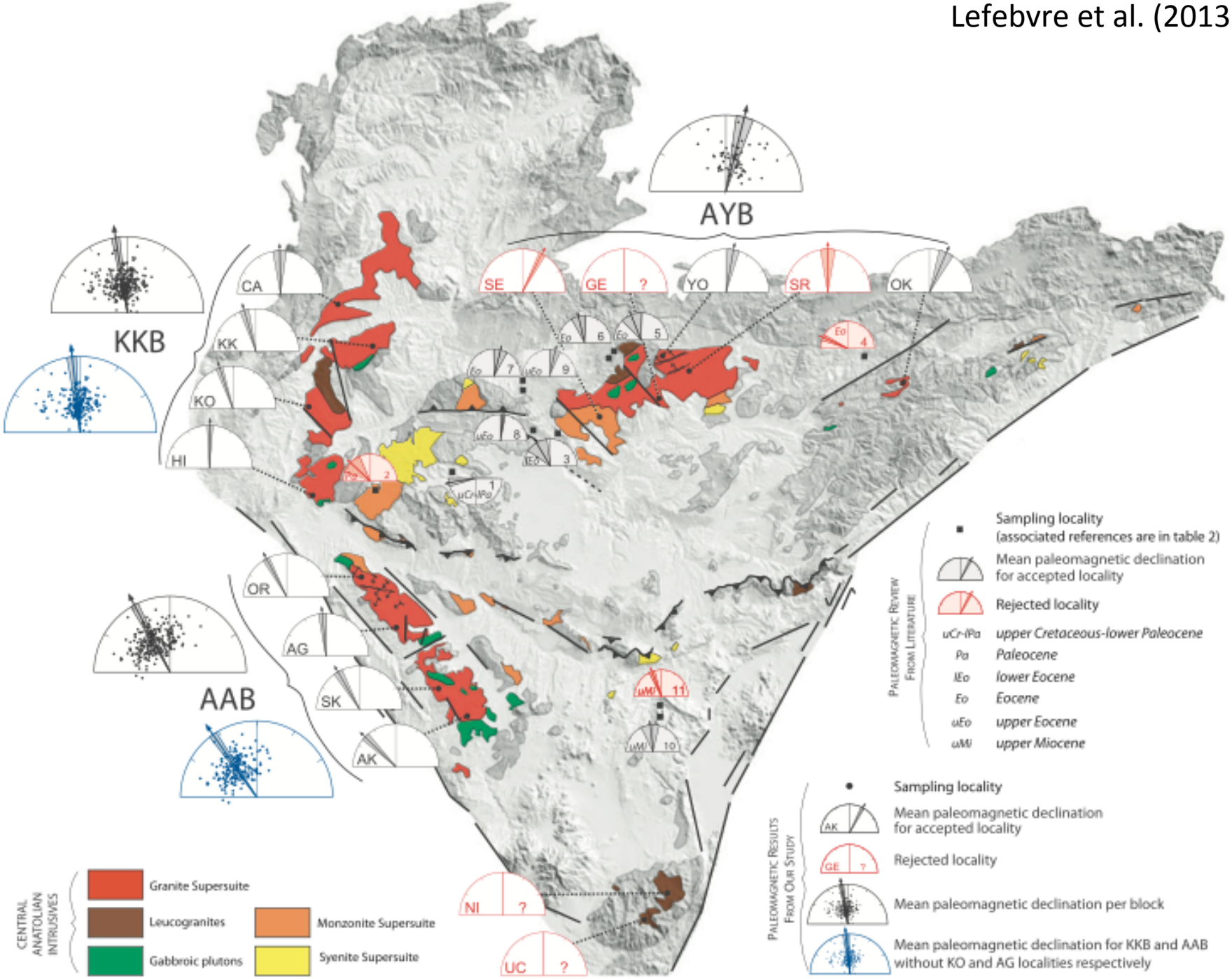

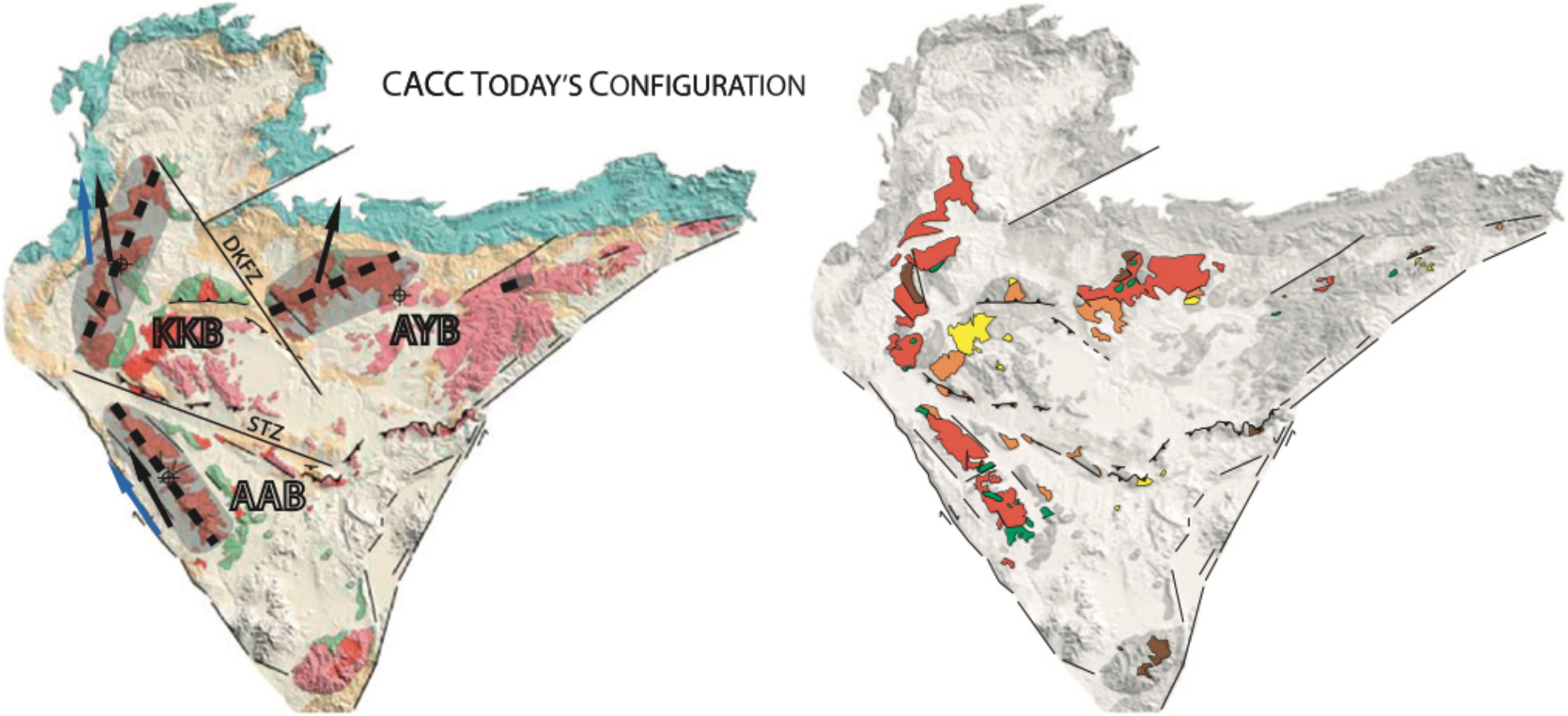

Lefebvre et al. (2013)

Possible Restorations

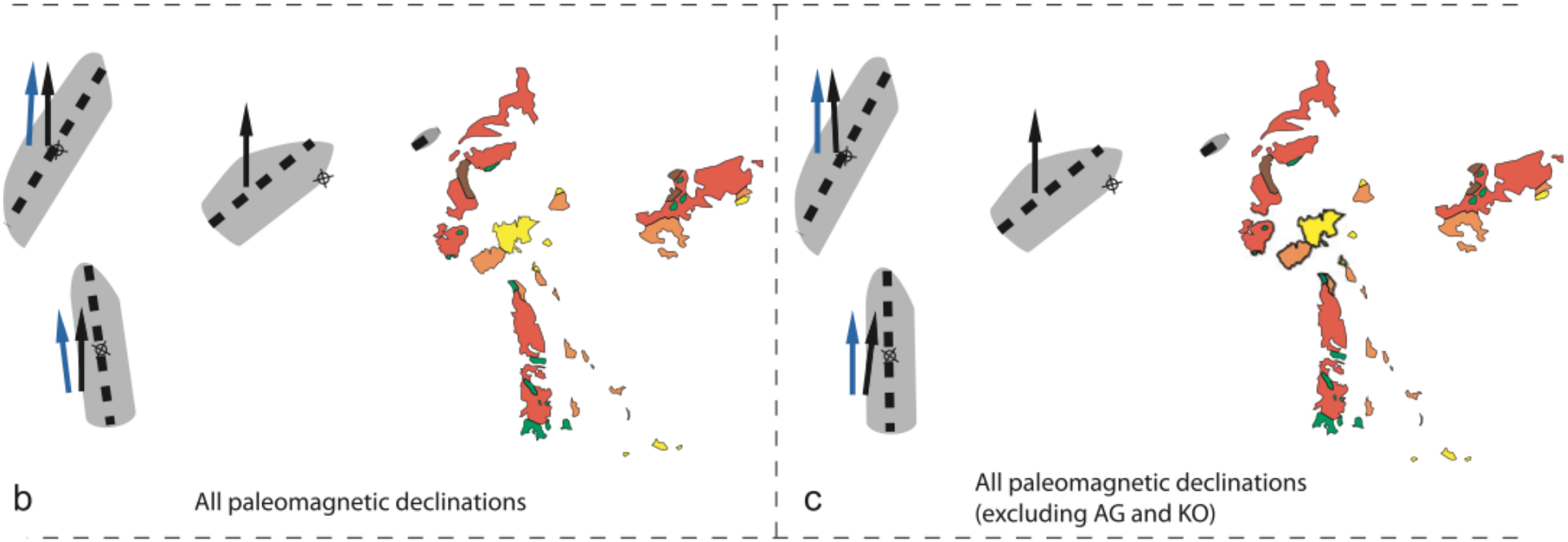

Lefebvre et al. (2013)

Possible Restorations

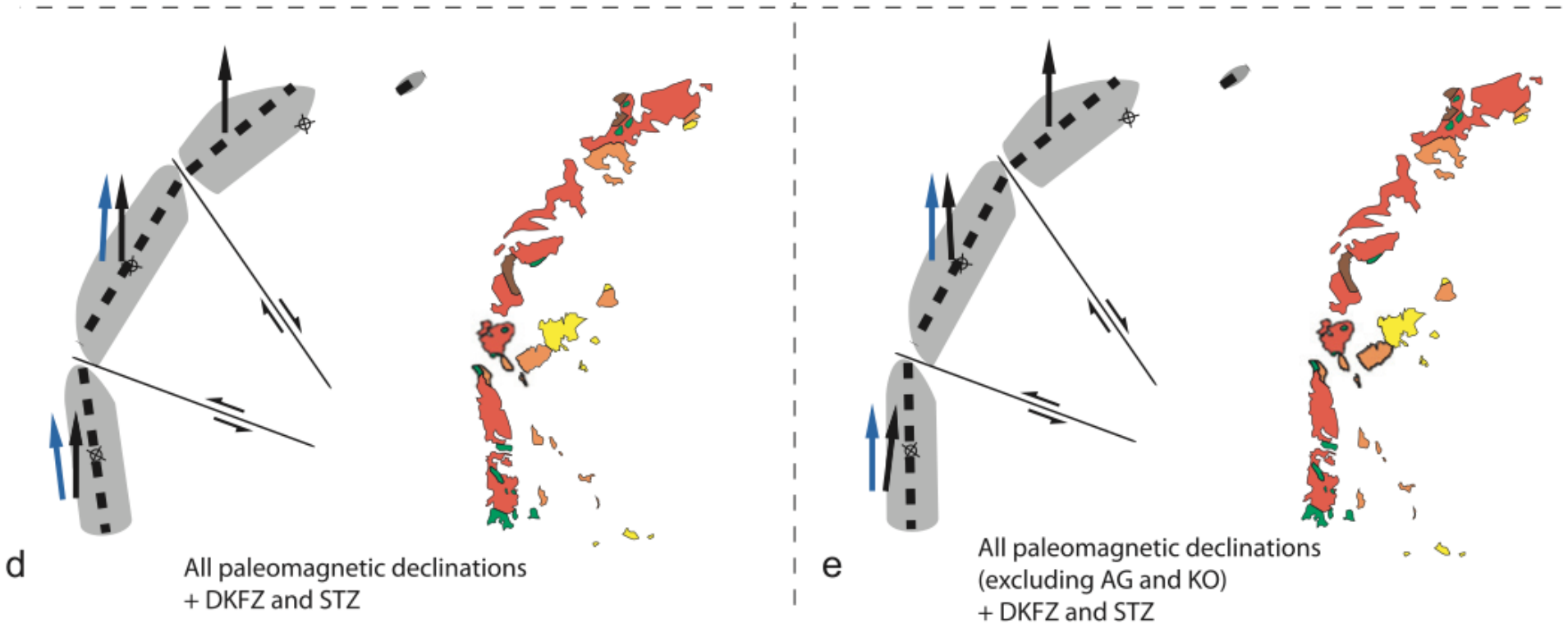

Lefebvre et al. (2013)

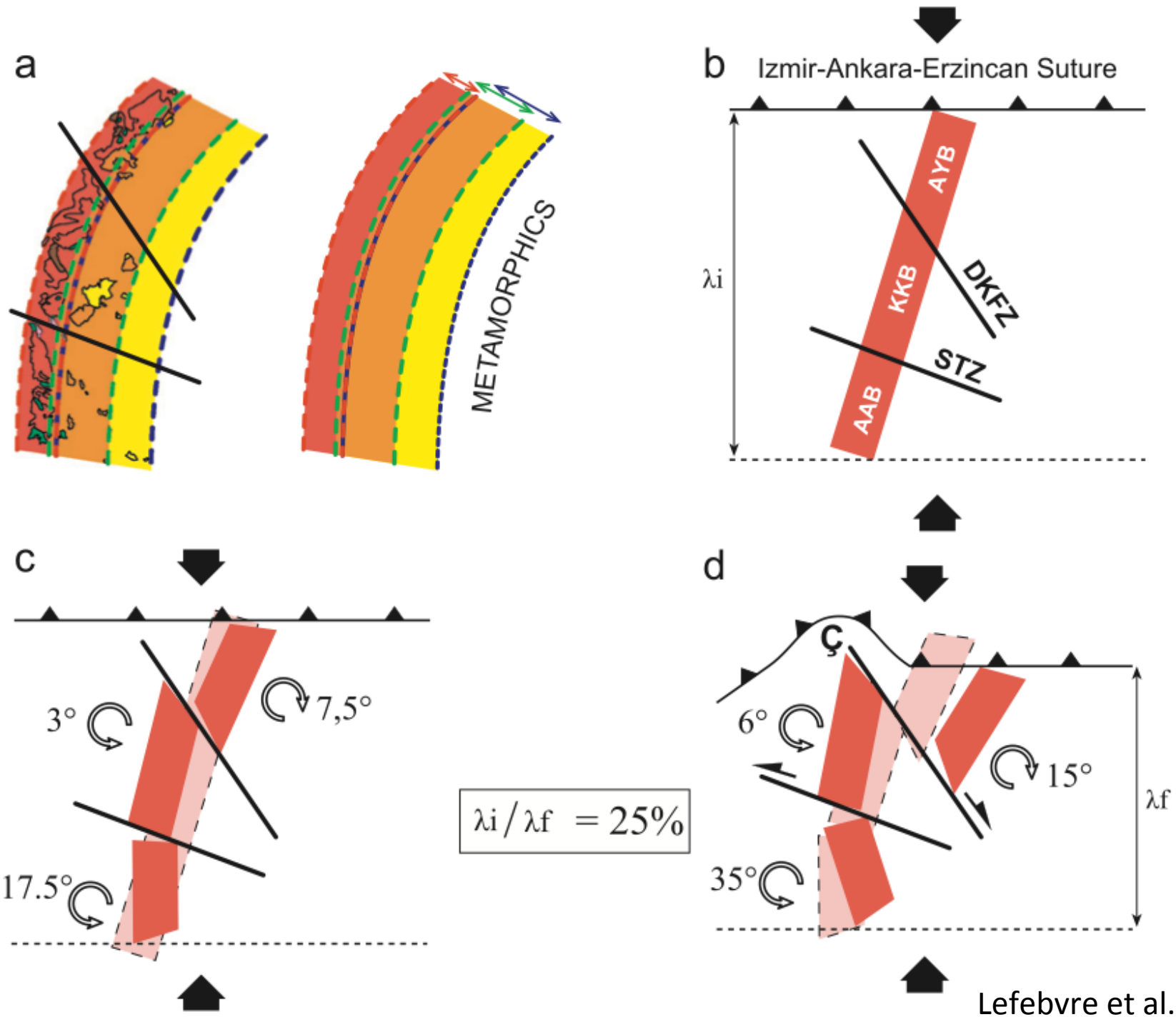

Lefebvre et al. (2013)

Conclusions

- Upper Cretaceous granitoids show rotations.
- The Akdag-Yozgat (AYB) shows ~15° CW rotation.
- The Kirsehir-Kirikkale block (KKB) shows ~6-9° CCW rotation.
- The Agacoren-Avanos block (AAB) shows ~28-35° CCW rotation.
- The blocks are separated by two transpressional strike-slip fault zones.
- Rotational and internal deformation in the CACC occurred throughout most of the Paleocene-Eocene.